

IV

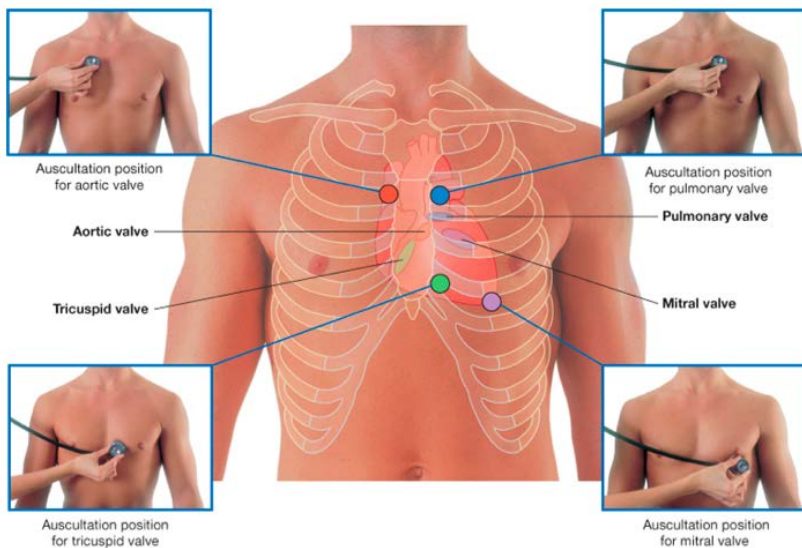
Modeling and Analysis of Heart Murmurs

Rajat Mittal, Jung Hee Seo, Hani Bakhshae, Chi Zhu
*Department of Mechanical Engineering &
Division of Cardiology*

Andreas Androu, Guillaume Garreau
Electrical Engineering

Johns Hopkins University

Cardiac Auscultation



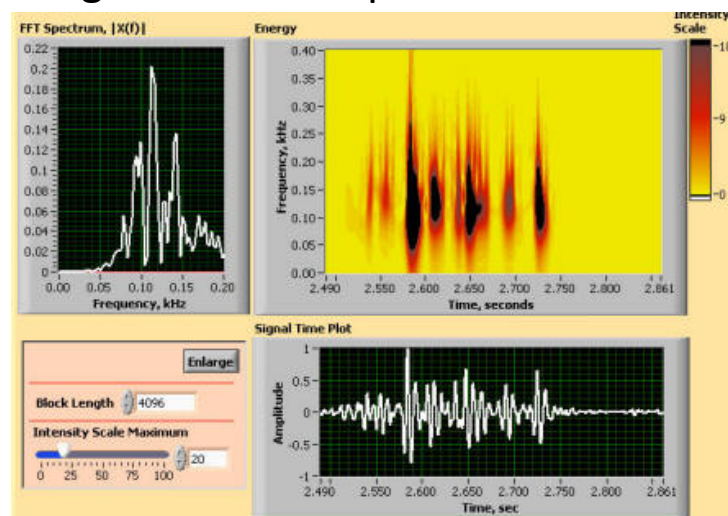
- 3000 year old technique
- Cheap
- Non-invasive, high sensitivity
- Good as a screening tool

But...

- Low specificity (high false positives) →
- Diagnosis is based on the empirical/statistical correlation
- Source mechanism of murmurs is poorly understood
- No modality provides simultaneous assessment of source and measurement

60% of all pediatric murmurs leading to referral are "innocent"

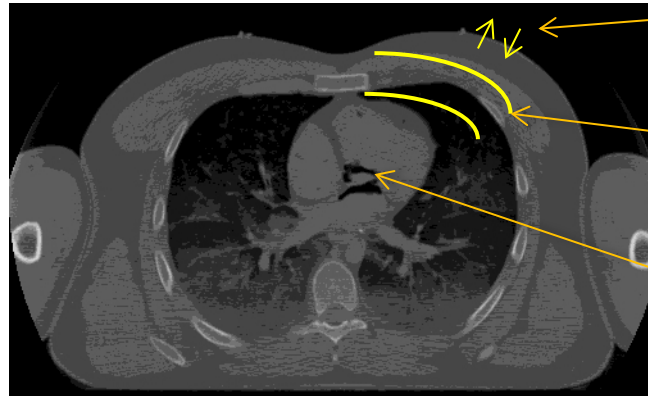
Digital Stethoscope



Murmur Scores	
Intensity	157.40
Duration	94.38
Frequency	118.43
Half Bandwidth	21.53
Murmur Grade	5

Computational Hemo-acoustics

Can computational modeling provide the missing link between cause (pathology) and effect (sound)?



Surface fluctuation on the chest

Structural wave Propagation

Pressure Fluctuation in the Heart

Computational Hemo-acoustics (CHA) directly simulate the above procedure:

- Prediction of murmur generation/propagation
- Source mechanism of murmurs
- Better Disease - Hemodynamics - Sound (Auscultation) relation

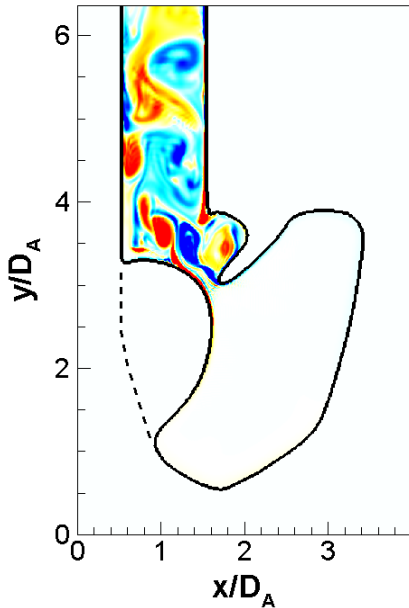
Present Approach:

-Immersed Boundary Method based Hybrid Approach

- **Blood Flow** - IBM Incompressible Navier-Stokes solver
- **Flow induced sound** - Linearized Perturbed Compressible Equations (LPCE)
- **Sound Propagation in tissue** – Linear wave equation

Computational Hemoacoustics

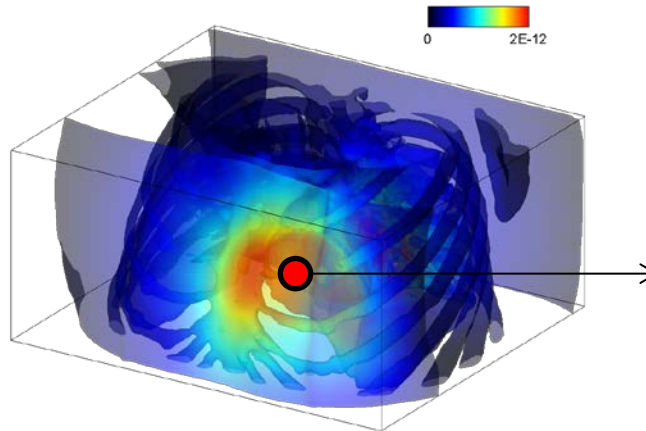
Hemodynamics



$P(\vec{x}, t)$

Hemodynamic
Sound Source

Wave Propagation

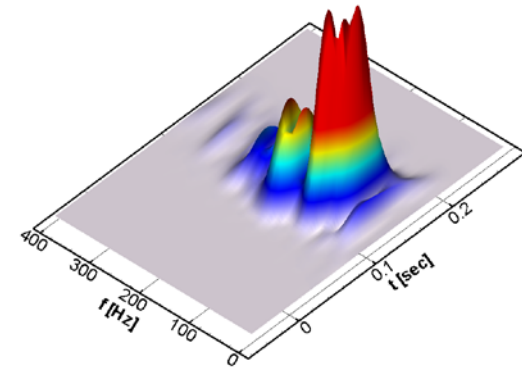
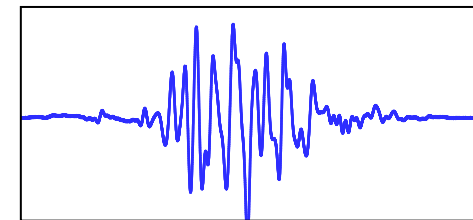


Structural wave Eqns.

$$\frac{\partial p_{ij}}{\partial t} + \lambda \frac{\partial u_k}{\partial x_k} \delta_{ij} + \mu \left(\frac{\partial u_i}{\partial x_j} + \frac{\partial u_j}{\partial x_i} \right) = S_p$$

$$\frac{\partial u_i}{\partial t} + \frac{1}{\rho} \frac{\partial p_{ij}}{\partial x_j} = \frac{\eta}{\rho} \frac{\partial}{\partial x_j} \left(\frac{\partial u_i}{\partial x_j} + \frac{\partial u_j}{\partial x_i} \right) + S_{u,i}$$

Sound Signal

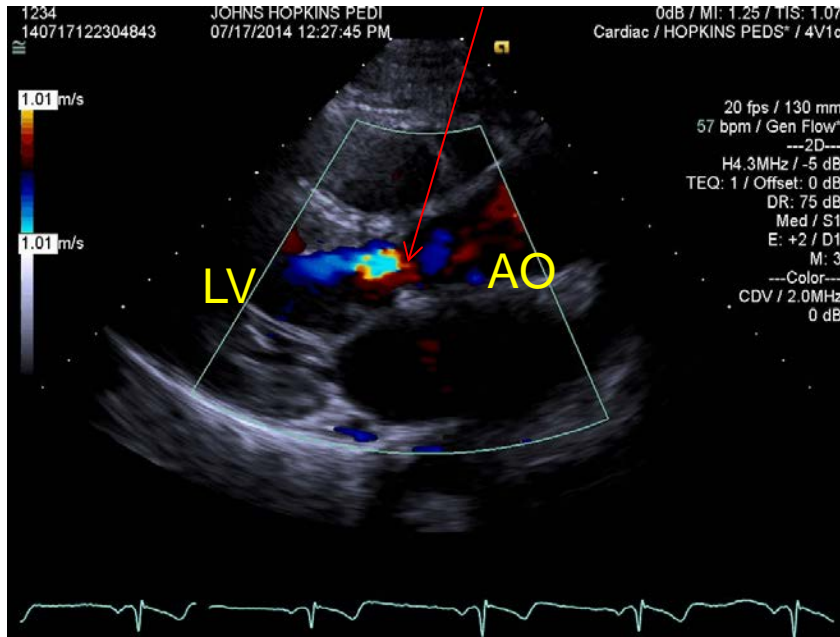


Incompressible N-S Eqns.

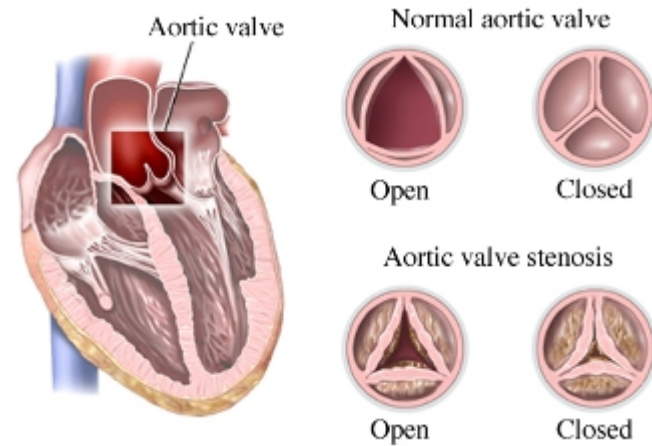
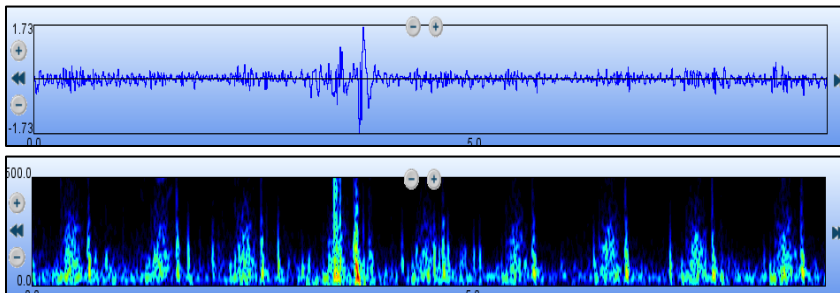
$$\nabla \cdot \vec{U} = 0, \quad \frac{D\vec{U}}{Dt} + \frac{1}{\rho_0} \nabla P = \nu_0 \nabla^2 \vec{U}$$

Murmur Associated with Aortic Stenosis

Aortic Valve Stenosis



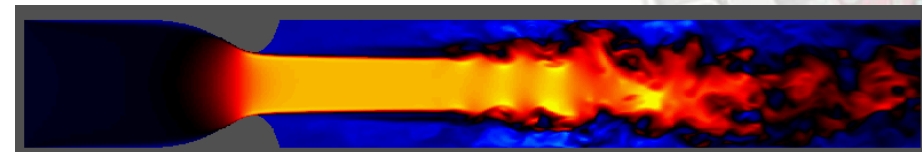
Aortic Stenosis Murmur



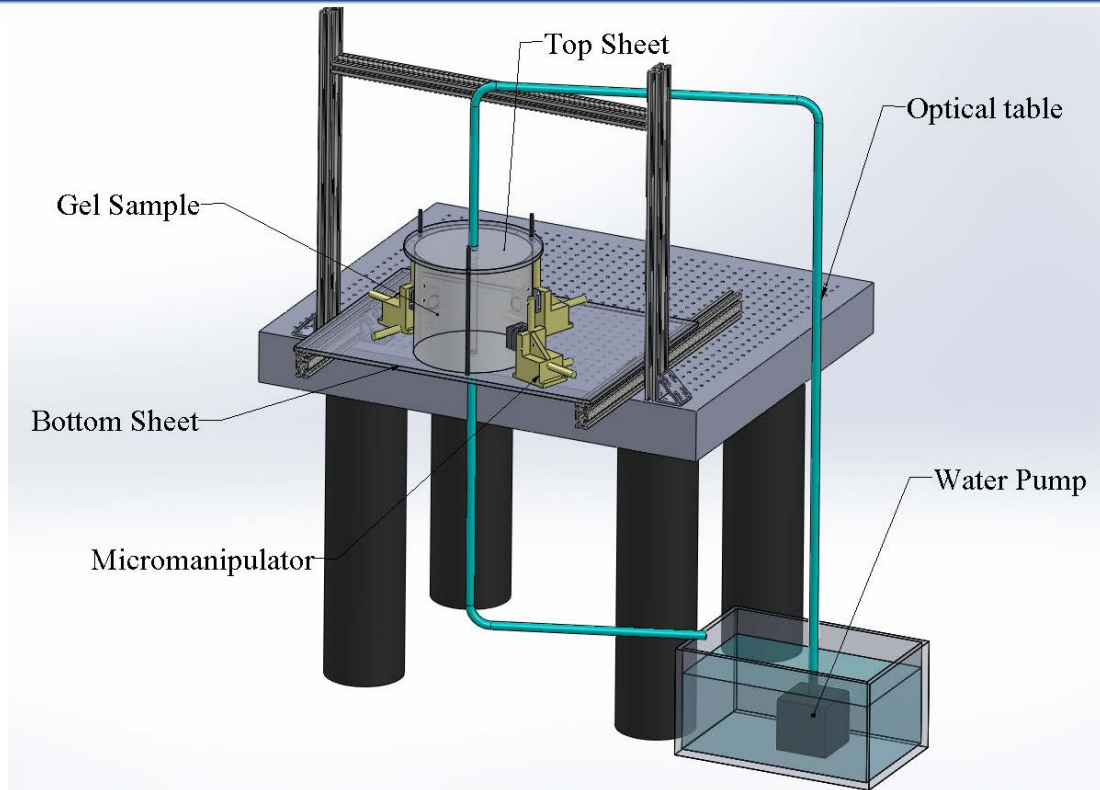
Simplified Hemodynamic Modeling



75% Aortic valve stenosis



Cardio-Thoracic Phantom Studies



Material: EcoFlex-10

$$\rho = 1040 \text{ kg/m}^3$$

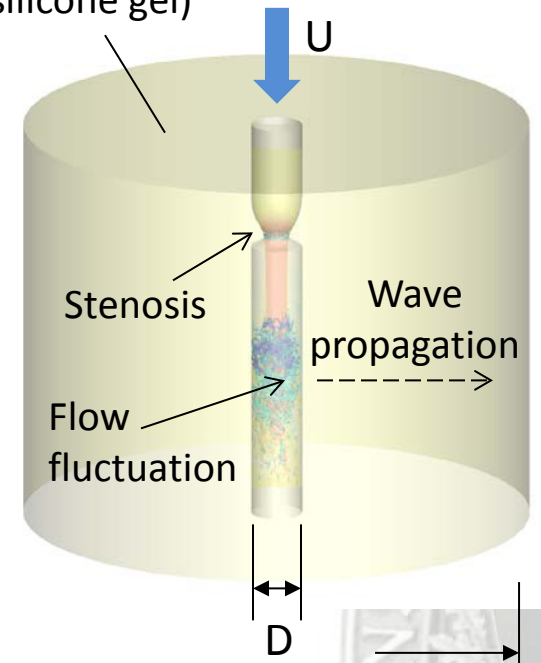
$$E = 55.16 \text{ kPa}$$

$$K = 91.3 \text{ Mpa} \quad (c_b = 297.3 \text{ m/s})$$

$$G = 18.39 \text{ kPa} \quad (c_s = 4.2 \text{ m/s})$$

$$\mu = 14 \text{ Pa s}$$

Thoracic phantom
(silicone gel)



$$U = 0.25 \text{ m/s}$$

$$D = 1.5875 \text{ cm}$$

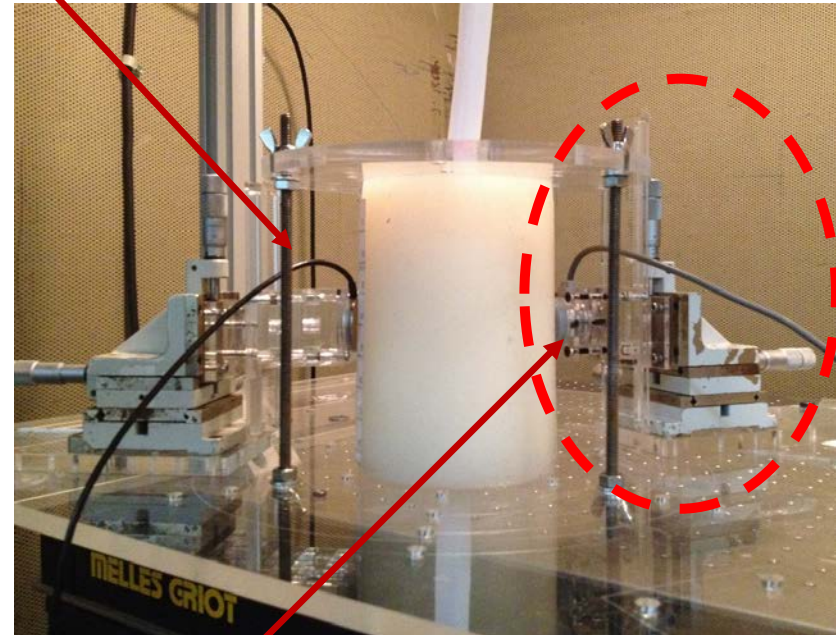
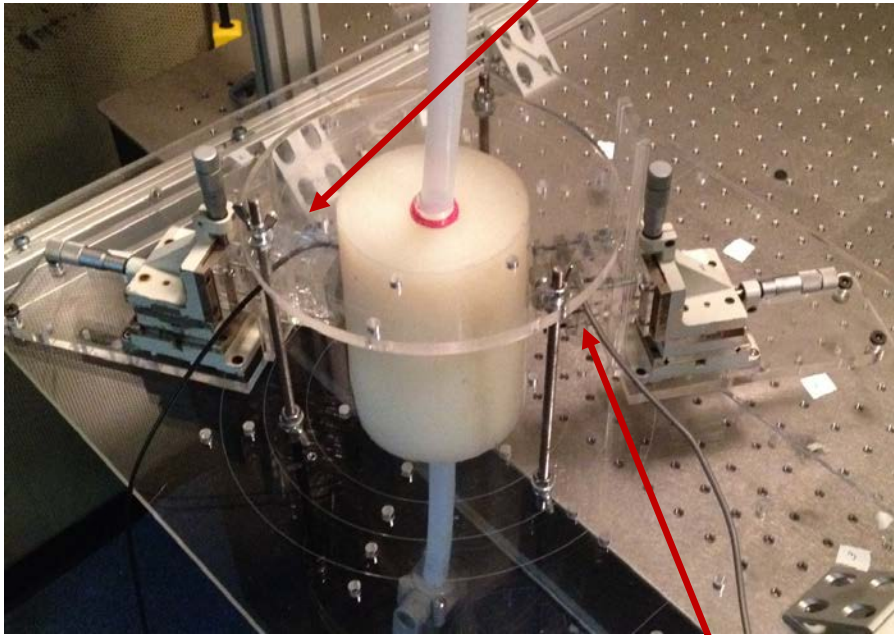
$$D_T = 9.84 \text{ cm}$$

$$Re = UD/\nu = 4000$$

$$St = fD/U$$

Acoustic Sensors

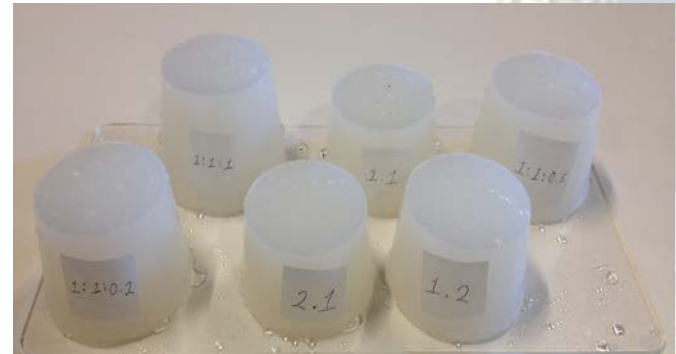
**Biopac sensor attached to the
Micromanipulator**



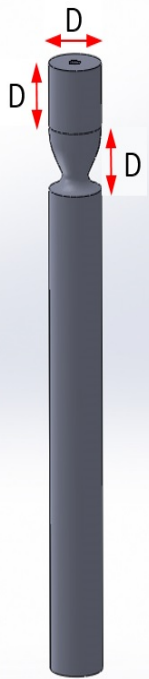
HP sensor attached to the Micromanipulator

Silicone Rubber- Tissue Mimicking Material

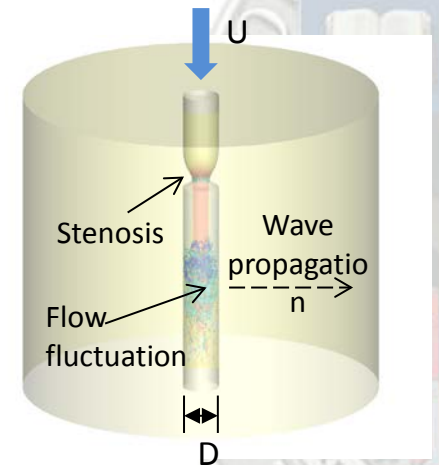
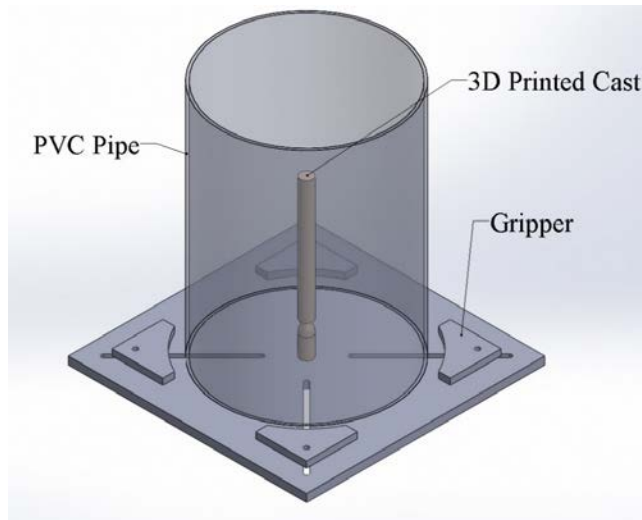
- Silicone rubber, Ecoflex 010 (Smooth-on)
 - Easy to produce
 - Extremely stable
 - Non-toxic and
 - Negligible shrinkage
- Procedure to make →
 - Mixing Part A part B,
 - Adding Silicon thinner,
 - Degassing for 3-4 min in (-29 in Hg) to remove air bubbles



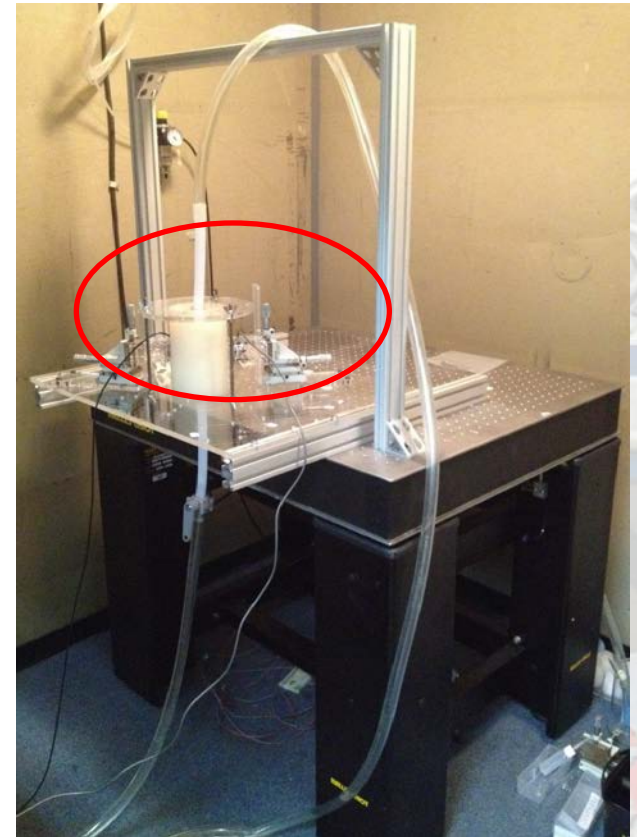
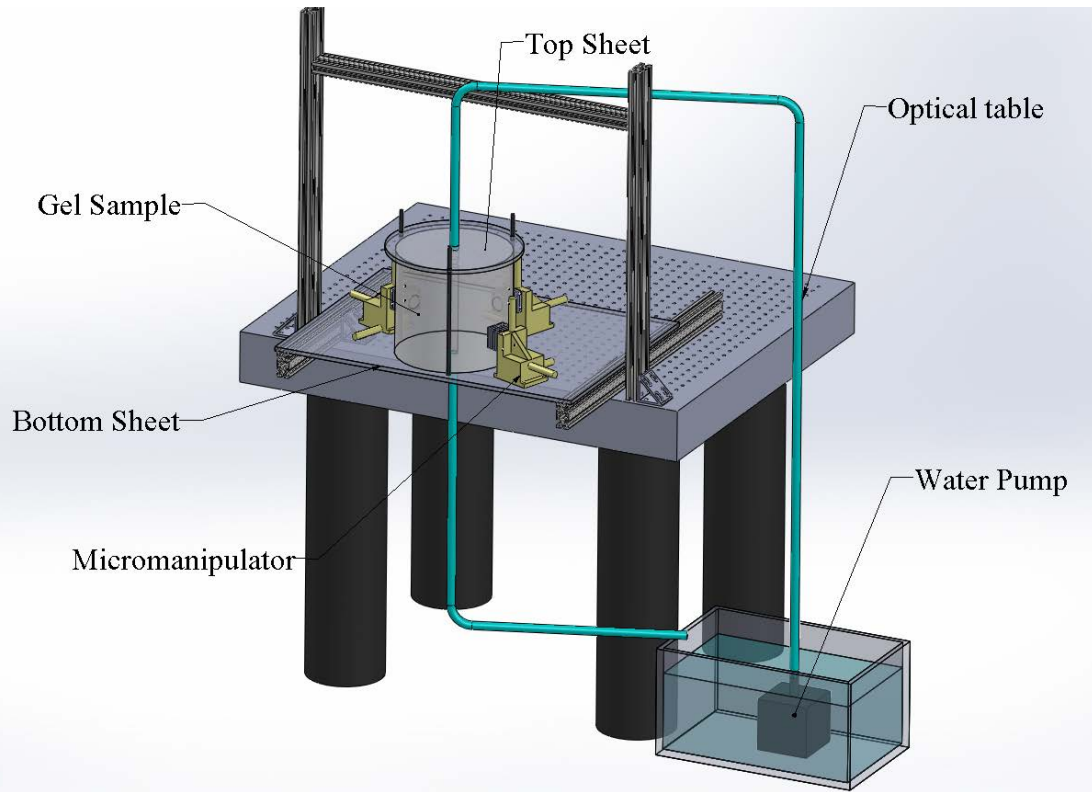
Murmur Generating



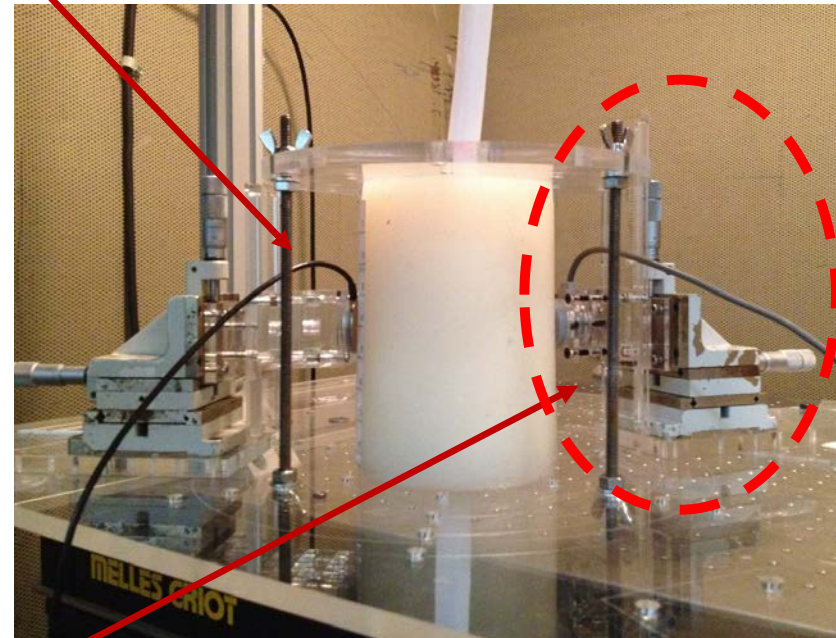
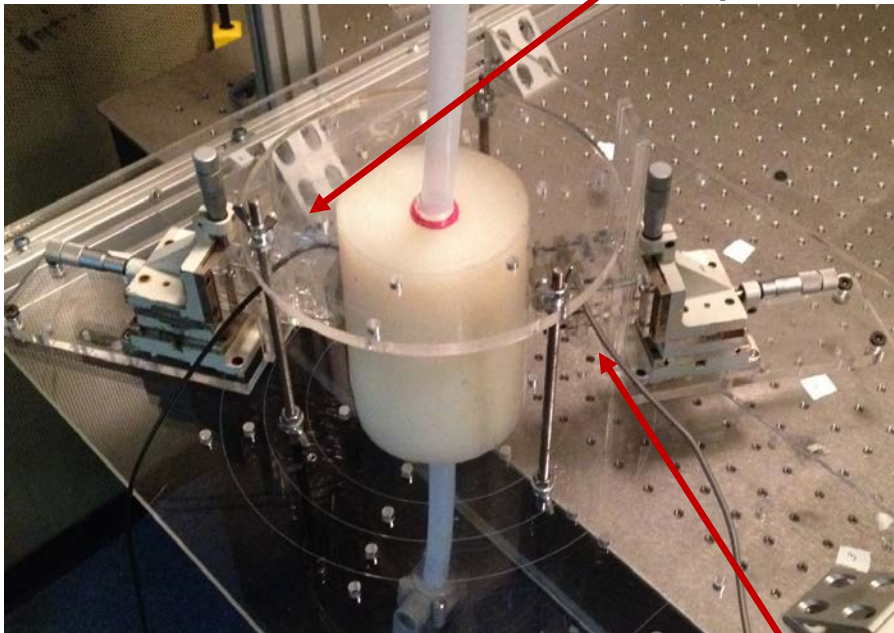
3D printed
Casts



Fluid Flow Circuit



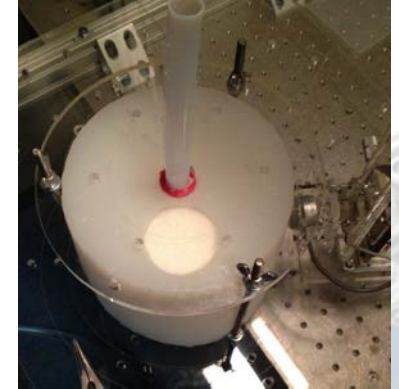
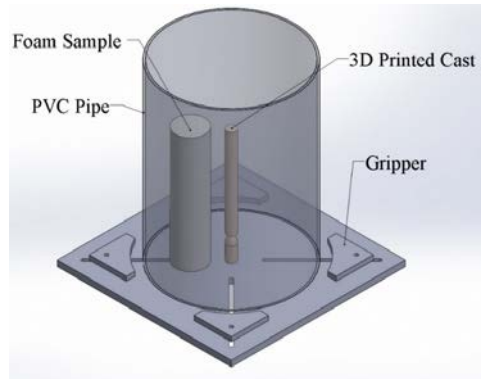
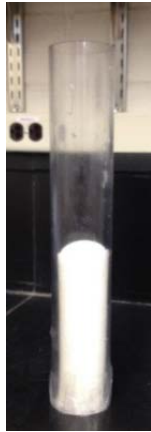
**Biopac sensor attached to the
Micromanipulator**



HP sensor attached to the Micromanipulator

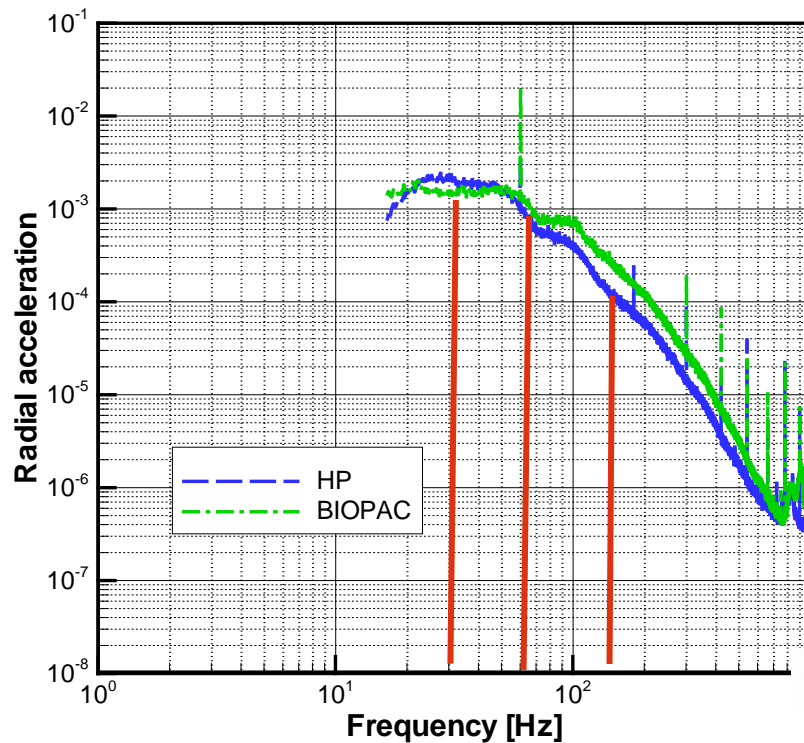
Cardiothoracic Phantom-2nd generation

- Adding lung to the phantom
- Foam is used to model the lung
- Non-axisymmetric model

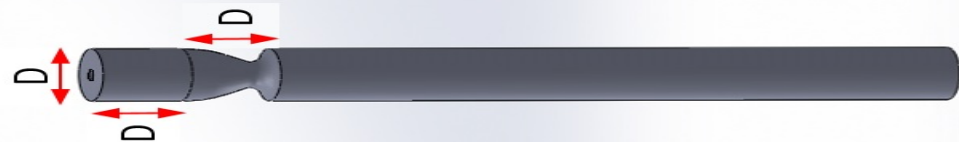
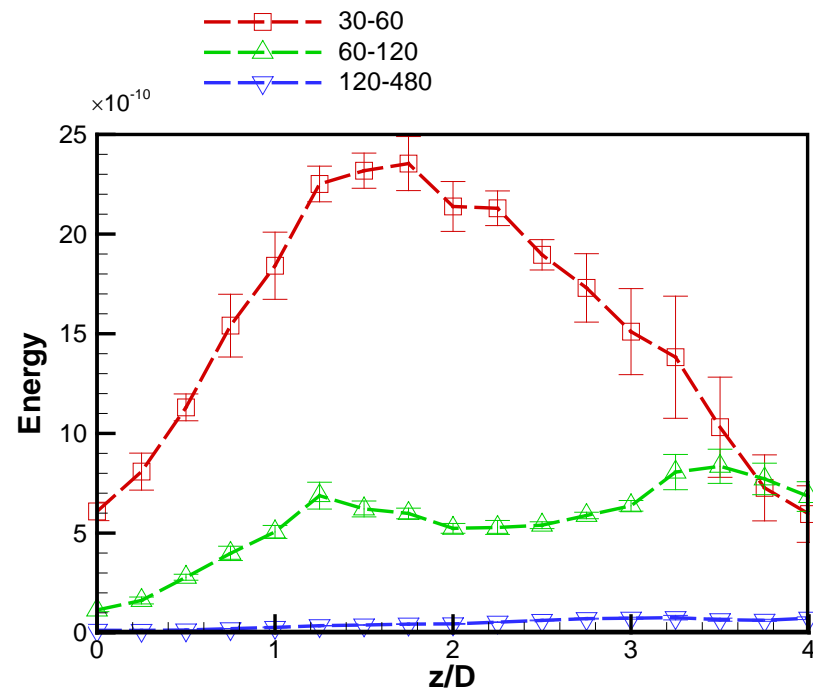


Experimental Measurements

Outer-surface radial accelerations



Frequency spectrum

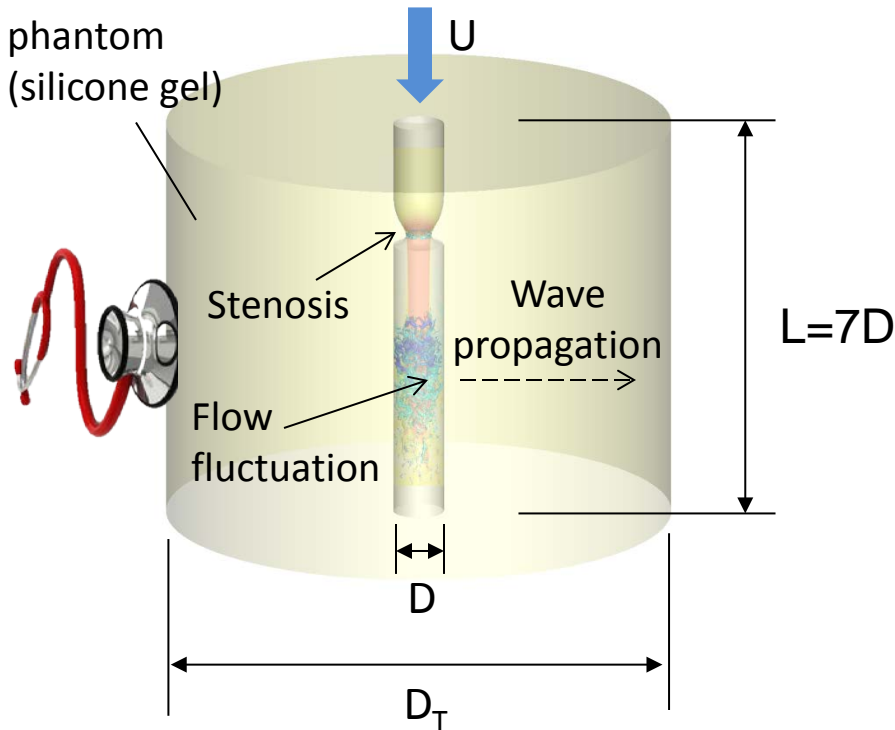


Energy mapping

Computational/Experimental Studies

Simple model for the aortic stenosis murmur

Thoracic phantom
(silicone gel)



$$Re = UD/\nu = 4000$$

Material properties:
Tissue mimicking,
viscoelastic gel (EcoFlex-10)

$$\rho = 1040 \text{ kg/m}^3$$

$$K = 1.04 \text{ GPa} \quad (c_b = 1000.0 \text{ m/s})$$

$$G = 18.39 \text{ kPa} \quad (c_s = 4.2 \text{ m/s})$$

$$\mu = 14 \text{ Pa s}$$

Other parameters:

$$U = 0.25 \text{ m/s}$$

$$D = 1.5875 \text{ cm}$$

$$D_T = 9.84 \text{ cm (gelA)}, 16.51 \text{ cm (gelB)}$$

c.f.

Biological soft tissue:

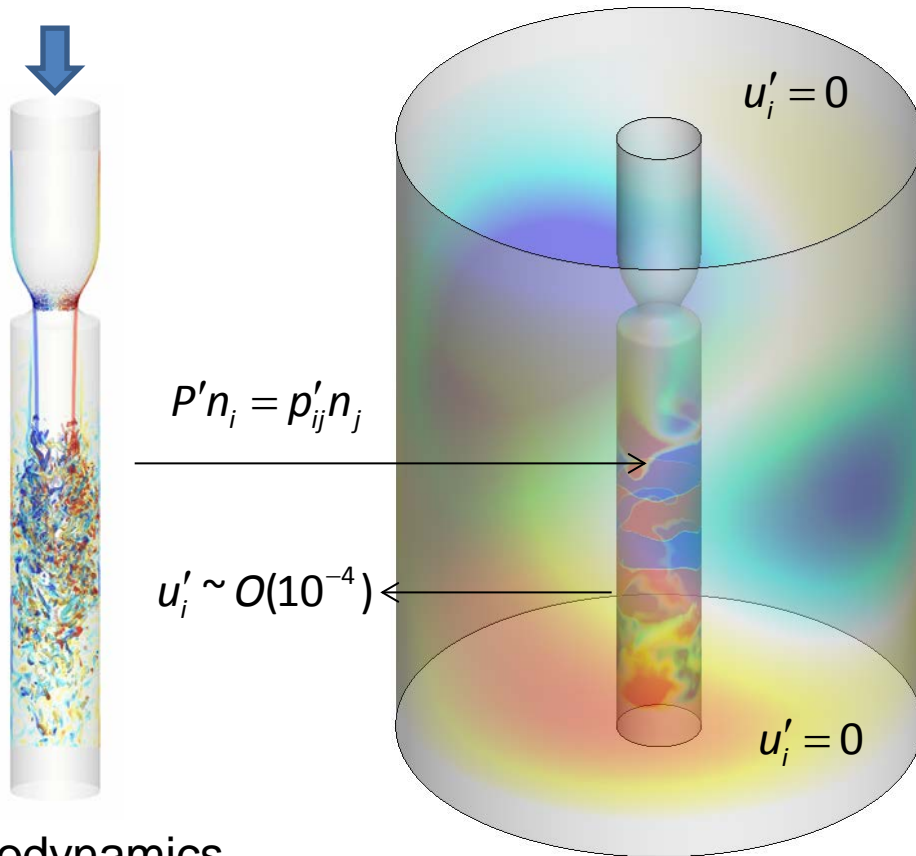
$$K = 2.25 \text{ GPa} \quad (c_b = 1500 \text{ m/s})$$

$$G = 0.1 \text{ MPa} \quad (c_s = 10 \text{ m/s})$$

$$\mu = 0.5 \text{ Pa s}$$



Computational Modeling



Hemodynamics
IBM, Incompressible N-S

$$\nabla \cdot \vec{U} = 0, \quad \frac{\partial \vec{U}}{\partial t} + (\vec{U} \cdot \nabla) \vec{U} + \frac{1}{\rho} \nabla P = \nu \nabla^2 \vec{U}$$

Elastic wave eq.
for viscoelastic material

Generalized Hooke's law
Kelvin-Voigt model

$$\frac{\partial p'_{ij}}{\partial t} + \lambda \frac{\partial u'_k}{\partial x_k} \delta_{ij} + \mu \left(\frac{\partial u'_i}{\partial x_j} + \frac{\partial u'_j}{\partial x_i} \right) = 0$$

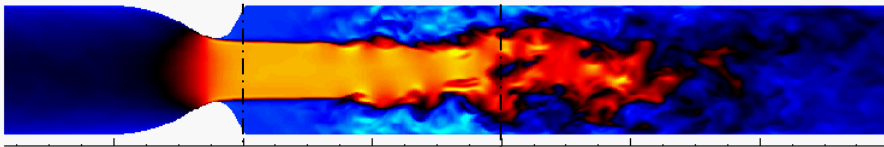
$$\frac{\partial u'_i}{\partial t} + \frac{1}{\rho} \frac{\partial p'_{ij}}{\partial x_j} = \frac{\eta}{\rho} \frac{\partial}{\partial x_j} \left(\frac{\partial u'_i}{\partial x_j} + \frac{\partial u'_j}{\partial x_i} \right)$$

High-order IBM,
6th order Compact Finite
Difference Scheme,
4 stage Runge-Kutta method

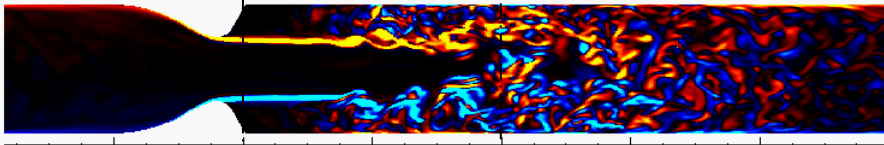
Flow Simulation

$Re_D=4000$

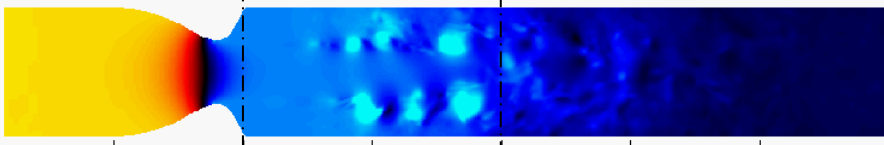
Axial velocity



Vorticity



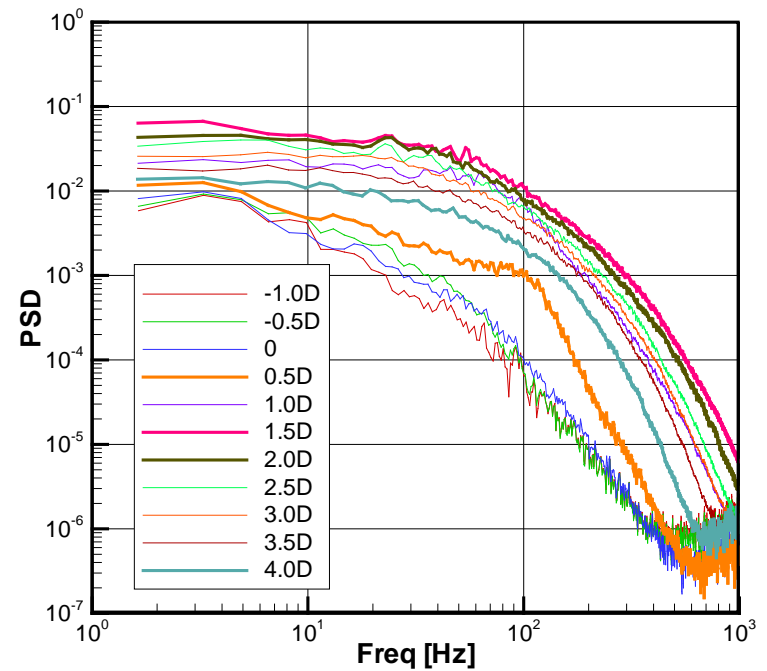
Pressure



0

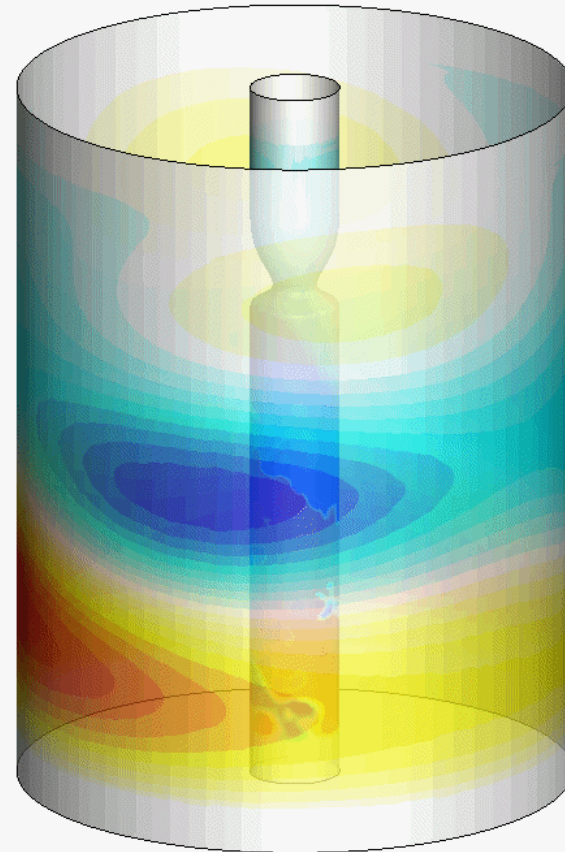
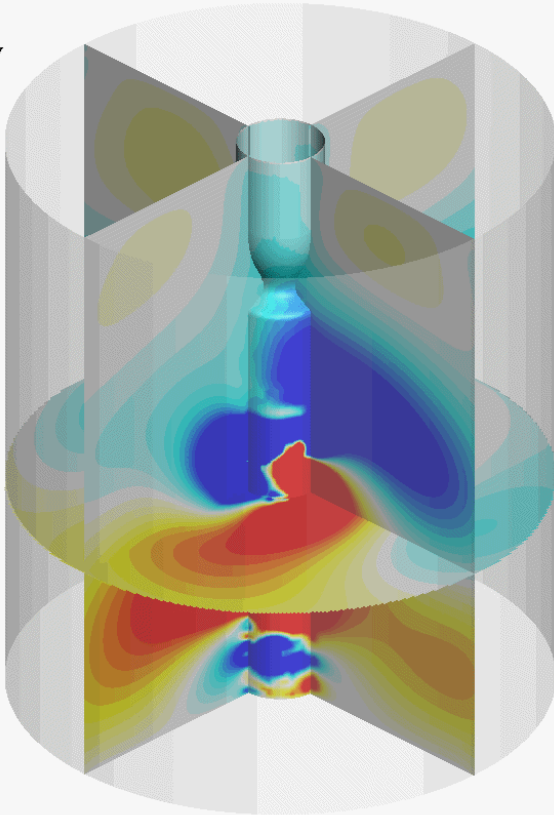
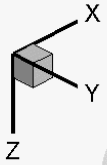
2D

Wall pressure spectrum



3D Elastic Wave Simulation

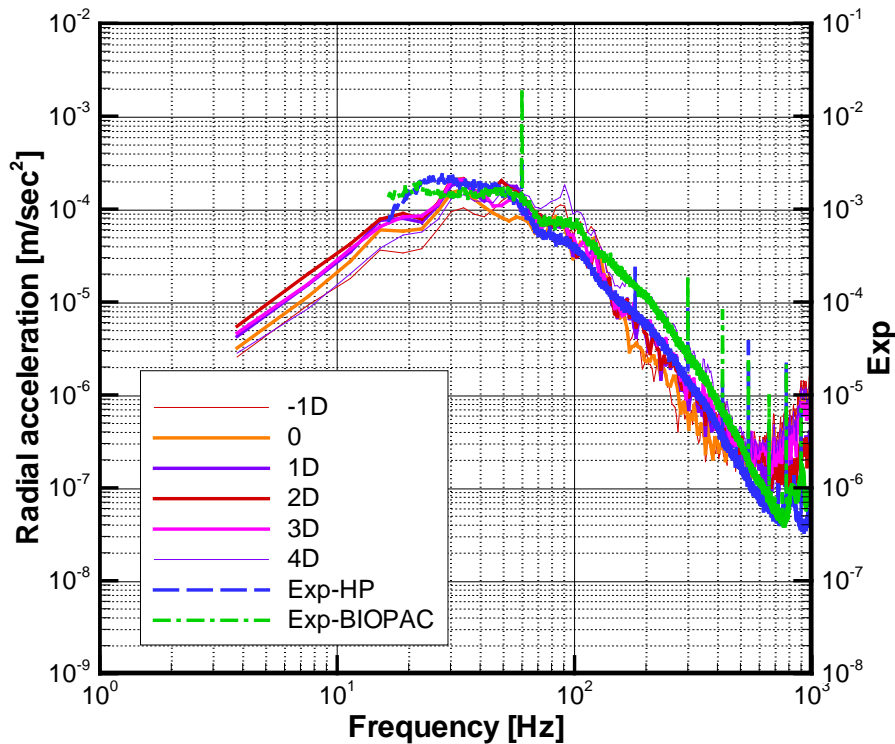
Radial velocity fluctuation contours



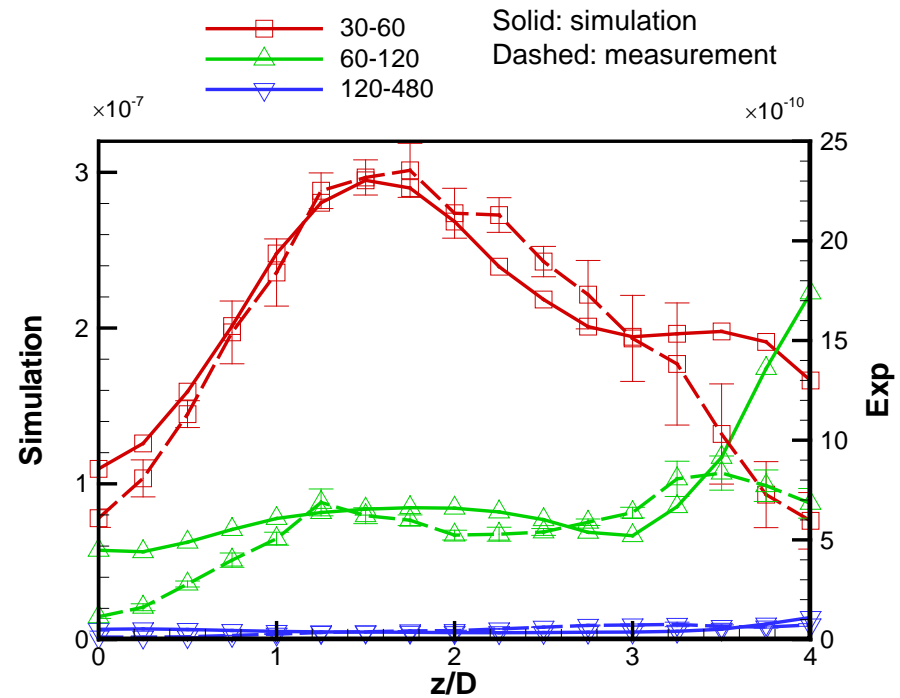
- 200x200x320 (12.8 M), about 60 hrs with 1024 cores for real time
0.8 sec

Comparison with Experimental Measurements

Outer-surface radial accelerations



Frequency spectrum



Energy mapping

Free-Space Green's Tensor

Analytical estimation of elastic wave solution
(no geometrical effects)

$$\rho \frac{\partial^2 u_i}{\partial t^2} - (\lambda \delta_{ij} \delta_{kl} + \mu (\delta_{ik} \delta_{jl} + \delta_{il} \delta_{jk})) \frac{\partial^2 u_l}{\partial x_j \partial x_k} = f_i(t) \delta(\vec{r})$$

$$u_i(t) = \frac{1}{2\pi} \int U_i(\omega) e^{-i\omega t} d\omega$$

$$f_i(t) = \frac{1}{2\pi} \int F_i(\omega) e^{-i\omega t} d\omega$$

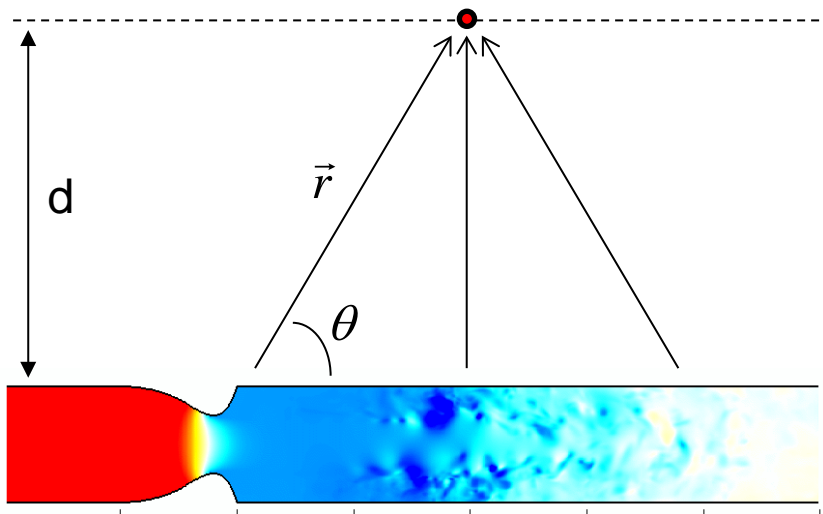
$$U_i(\vec{r}, \omega) = G_{ij}(\vec{r}, \omega) F_j(\omega)$$

Green's tensor (Ben-Menahem & Singh, 1981)

$$G_{ij}(\vec{r}, \omega) = \frac{ik_p}{12\pi(\lambda + 2\mu)} \left(\delta_{ij} h_0^{(1)}(k_p r) + (\delta_{ij} - 3 \frac{x_i x_j}{r^2}) h_2^{(1)}(k_p r) \right) - \frac{ik_s}{12\pi\mu} \left(-2\delta_{ij} h_0^{(1)}(k_s r) + (\delta_{ij} - 3 \frac{x_i x_j}{r^2}) h_2^{(1)}(k_s r) \right)$$

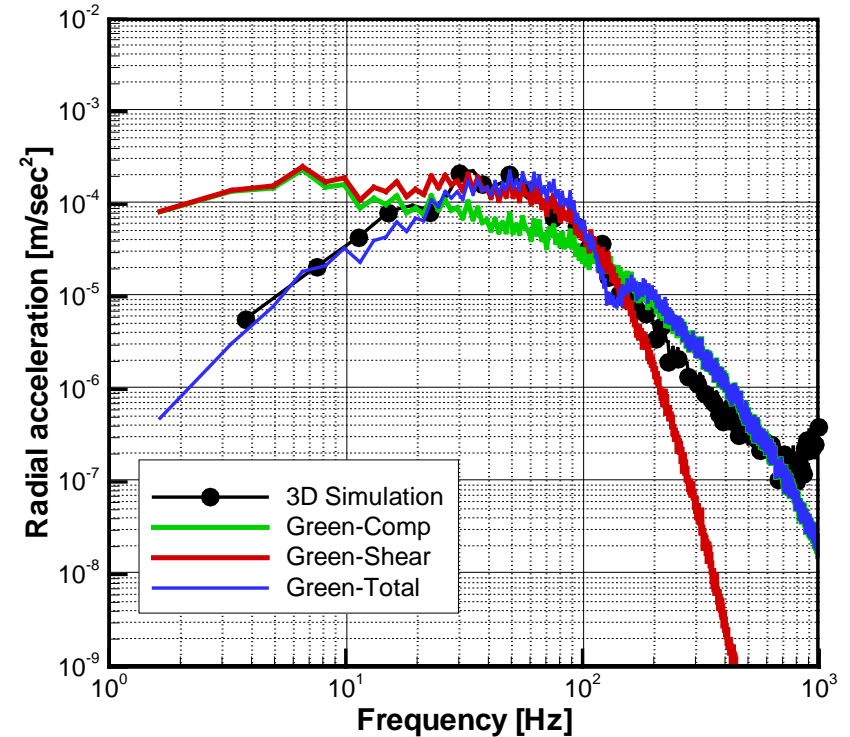
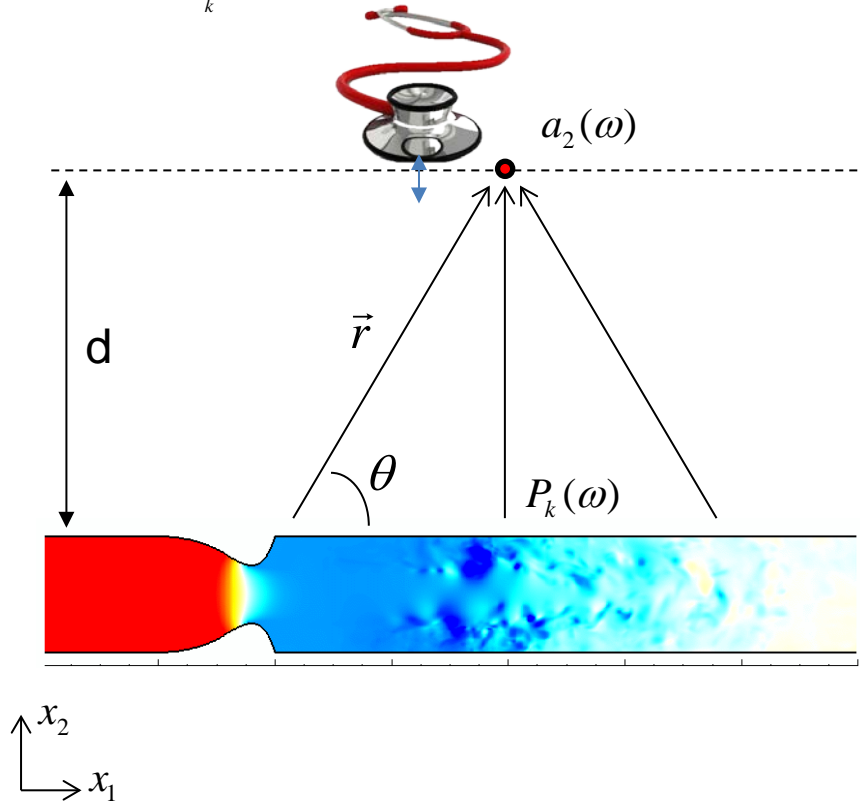
$$k_p = \omega / c_p, \quad c_p = \sqrt{(\lambda + 2\mu) / \rho}$$

$$k_s = \omega / c_s, \quad c_s = \sqrt{\mu / \rho}$$



Evaluation of Radial Acceleration

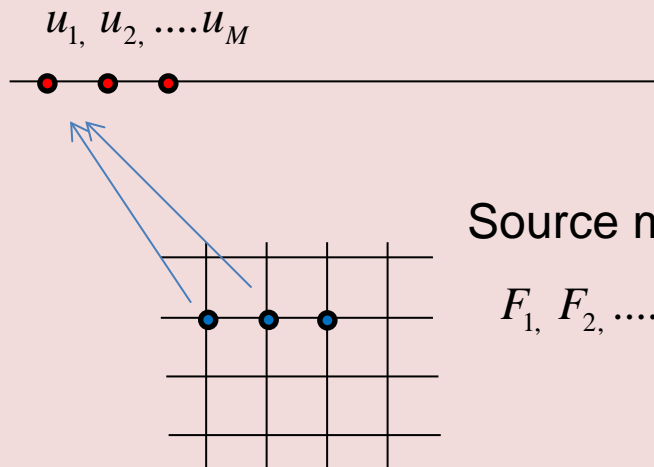
$$a_m(\vec{r}, \omega) = \sum_k (i\omega)^2 G_{m,k}(\vec{r}_k, \omega) F_{n,k}(\omega), \quad F_{2,k}(\omega) = P_k(\omega) \Delta A$$



Oblique shear waves contribute significantly to the stethoscopic signal!

Source Localization

Surface measurements



$$u_m = \sum_{n=1}^N G(x_m; x_n) F_n$$

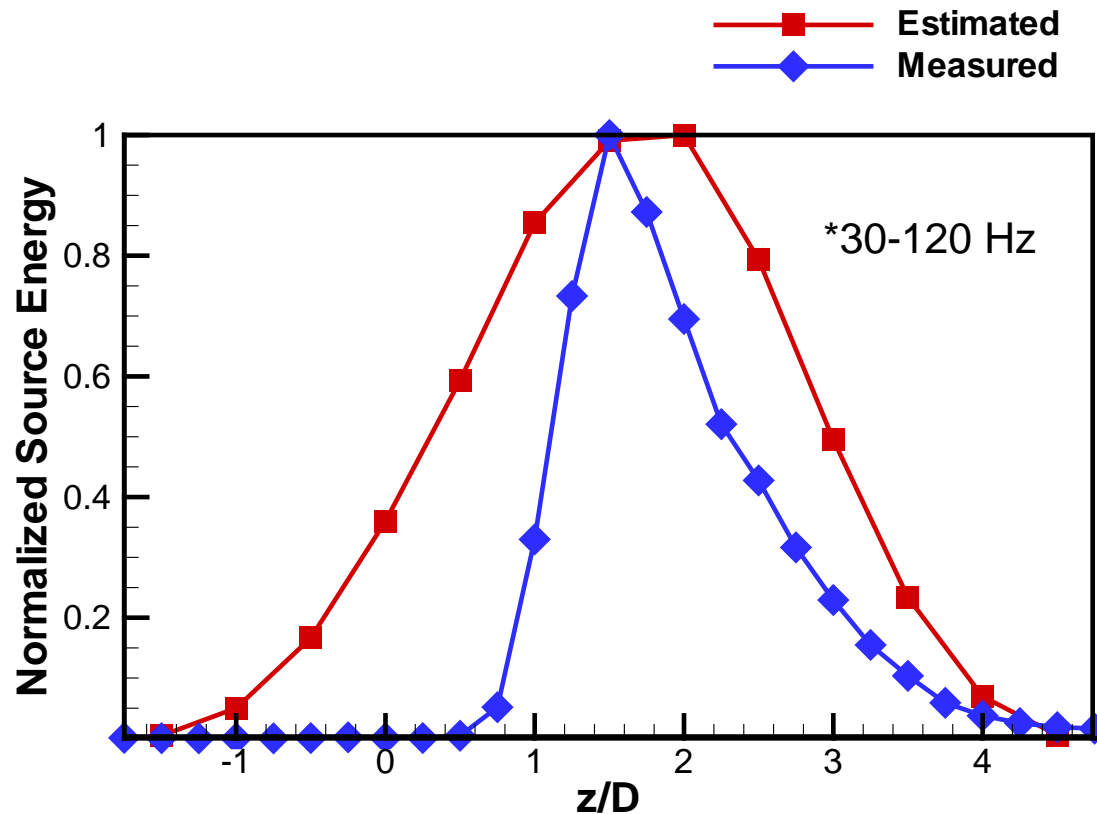
$$\begin{bmatrix} u_1 \\ \vdots \\ u_M \end{bmatrix} = \mathbf{G} \begin{bmatrix} F_1 \\ \vdots \\ F_N \end{bmatrix}$$

\mathbf{G} : M by N complex matrix

$$[F] = \mathbf{G}^+ [u]$$

\mathbf{G}^+ : Pseudo inverse of \mathbf{G}

Source Localization



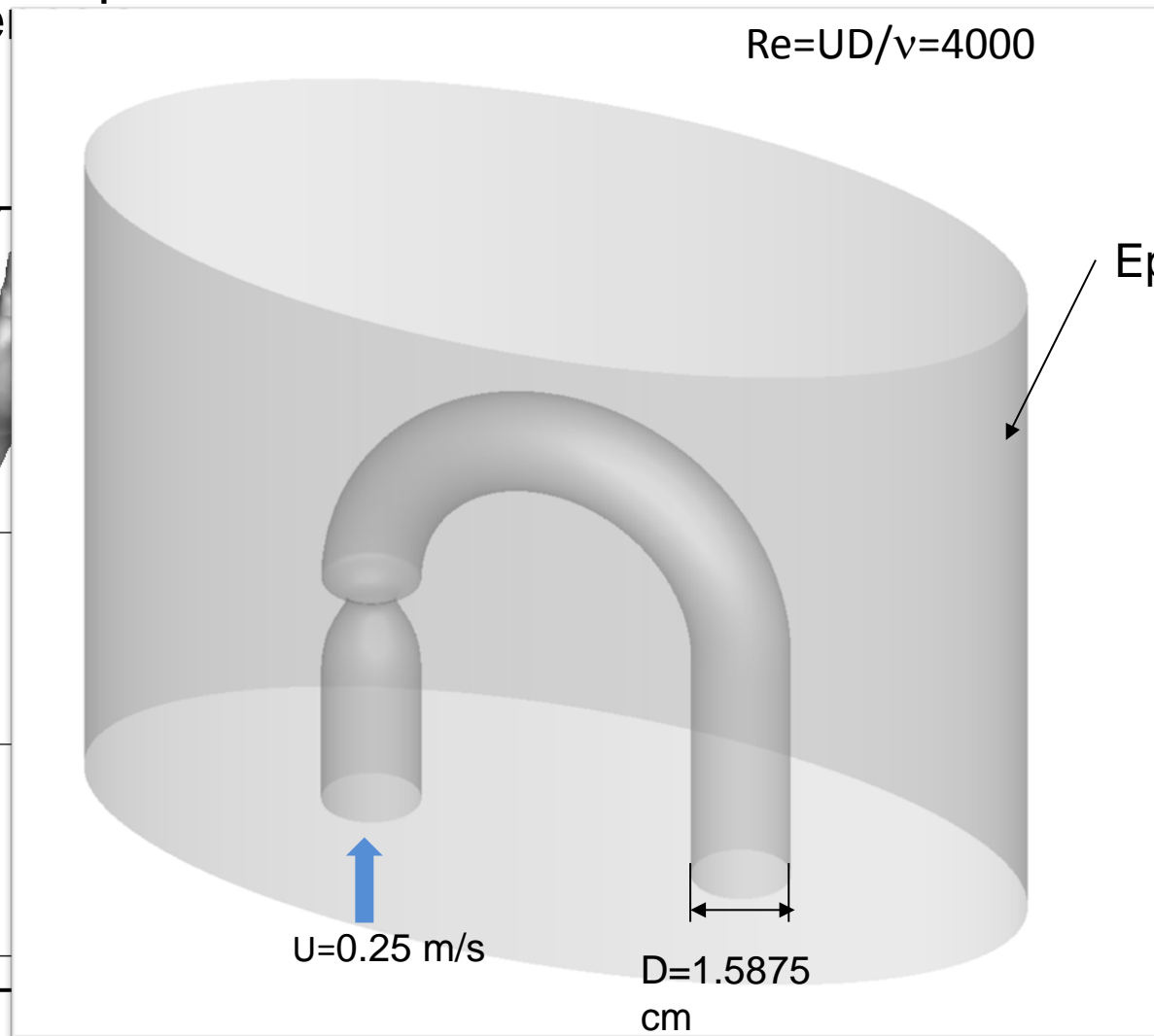
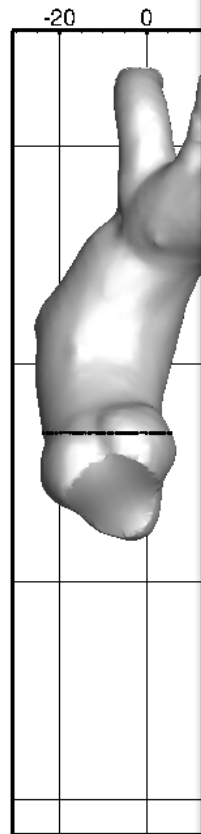
Proceeding towards using a multi-sensor stethoscopic array (StethoVest) for automatic murmur localization



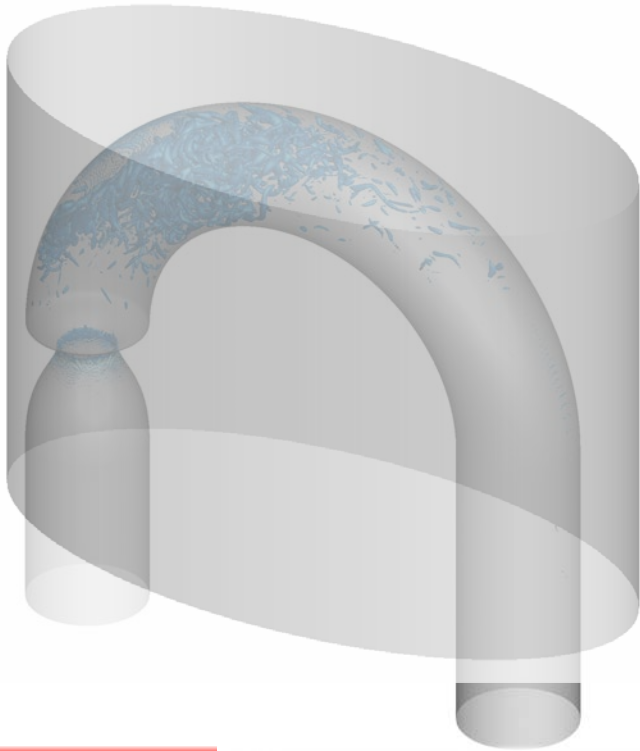
Computational Modeling

Aortic stenosis

Patient



Computational Modeling



Fluid Solver: Vicar Code, sharp interface IBM

$$\frac{\partial U_i}{\partial t} + U_j \frac{\partial U_i}{\partial x_j} = -\frac{1}{\rho_f} \frac{\partial P}{\partial x_i} + \nu \frac{\partial^2 U_i}{\partial x_j^2}$$

$$\frac{\partial U_i}{\partial x_i} = 0.$$

See: Mittal, R., *et al.*, JCP, 2008

Acoustic Solver:

$$\frac{\partial p_{ij}}{\partial t} + \lambda \frac{\partial v_k}{\partial x_k} \delta_{ij} + \mu \left(\frac{\partial v_i}{\partial x_j} + \frac{\partial v_j}{\partial x_i} \right) = 0$$

$$\frac{\partial v_i}{\partial t} + \frac{1}{\rho_s} \frac{\partial p_{ij}}{\partial x_j} = \frac{\eta}{\rho_s} \frac{\partial}{\partial x_j} \left(\frac{\partial v_i}{\partial x_j} + \frac{\partial v_j}{\partial x_i} \right).$$

v_i – structure velocity.

λ, μ – 1st and 2nd Lamé's constants.

ρ_s – density.

K – bulk modulus, = 1.04 GPa.

G – shear modulus, = 18.39 KPa.

η – viscosity, = 14.0 Pa s.

Numerical methods:

Interior nodes:

6th – order compact scheme

Immersed boundary:

approximating polynomial method

Time advancement:

4th – order Runge-Kutta method

See: Seo, J. H., & Mittal, R., JCP, 2011

Hemodynamic Simulation Results

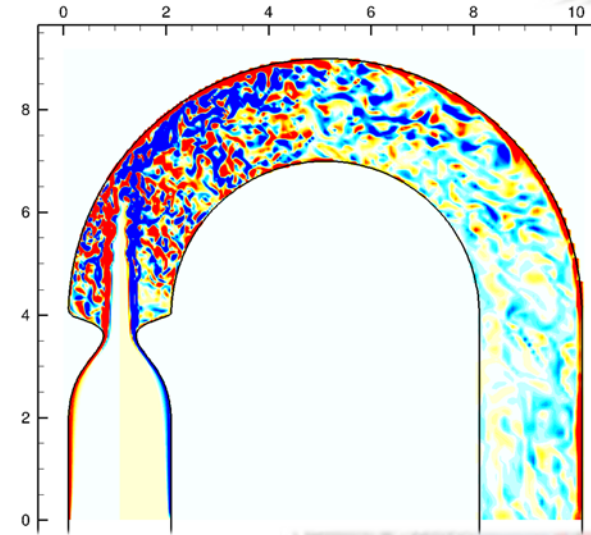
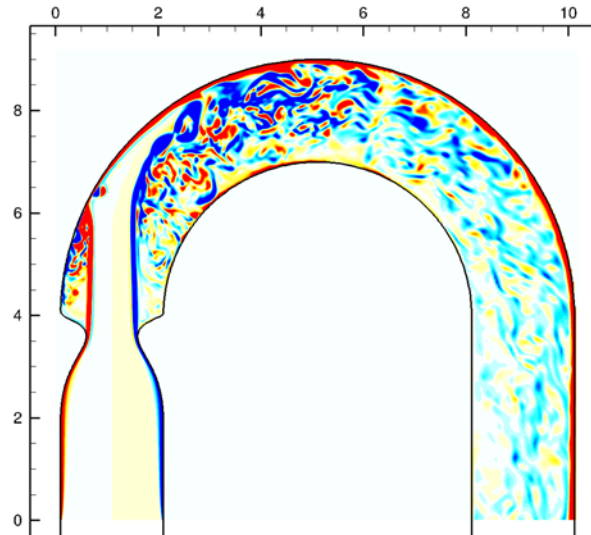
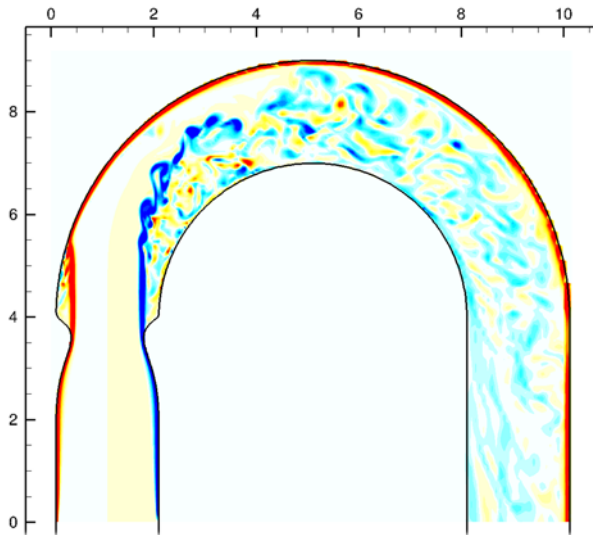
x component of vorticity

Same contour level

50%

75%

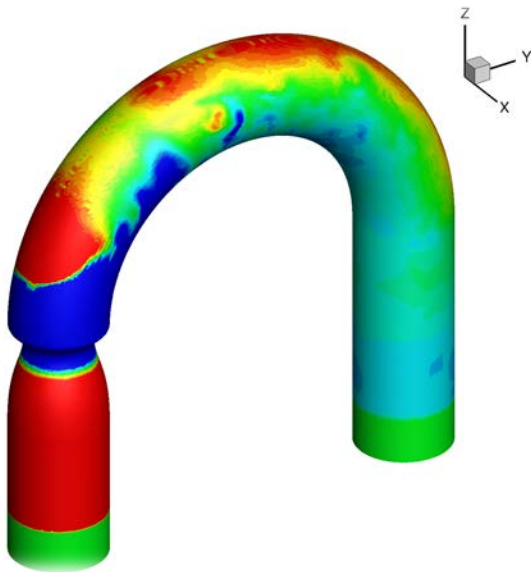
90%



Hemodynamic Simulation Results

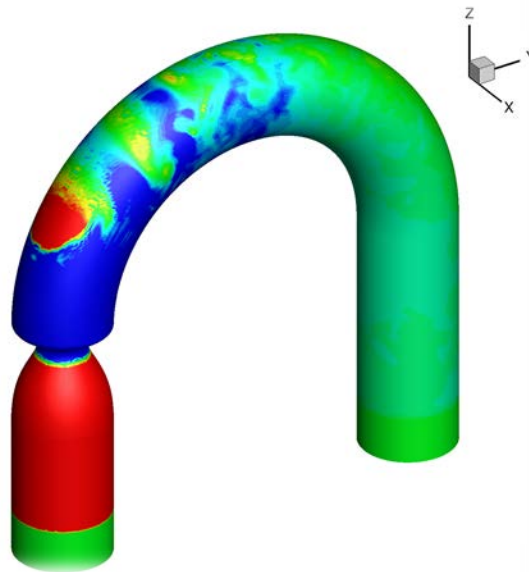
Contour of surface pressure

50%



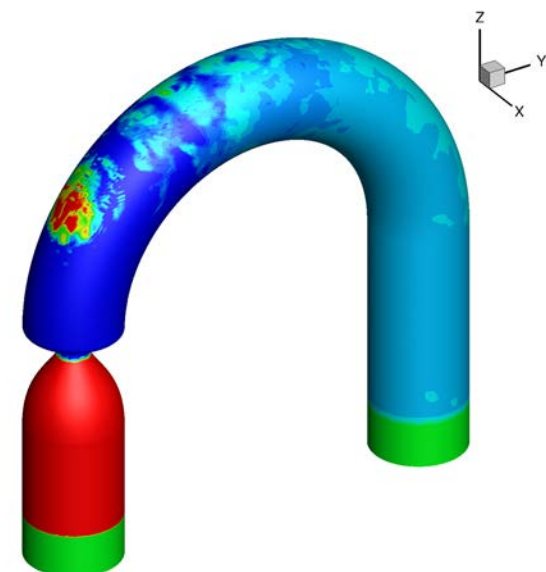
5 times smaller
contour level

75%



Baseline

90%

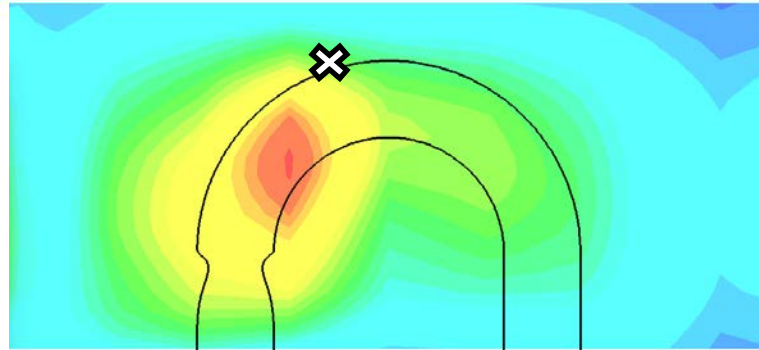


5 times larger
contour level

Source Location

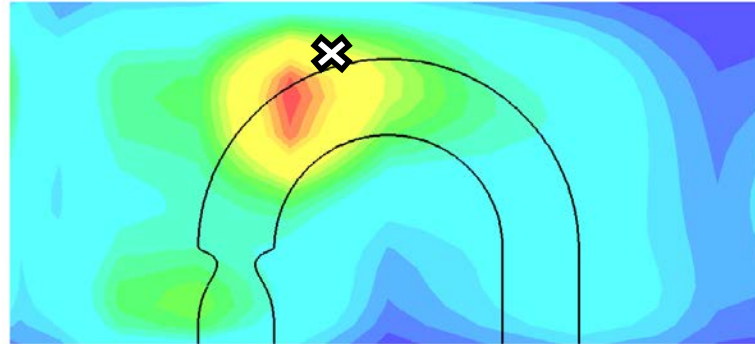
Surface Signal

50%



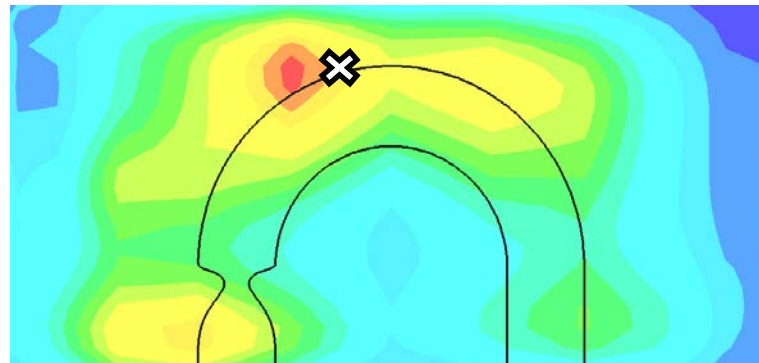
1000 times smaller
contour level

75%



Baseline

90%



100 times larger
contour level

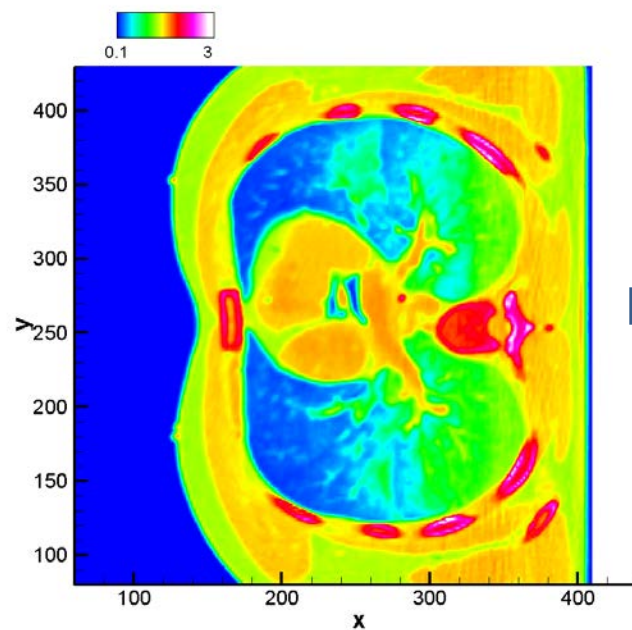
Realistic Thorax Model

Need to account for thoracic structures on sound propagation

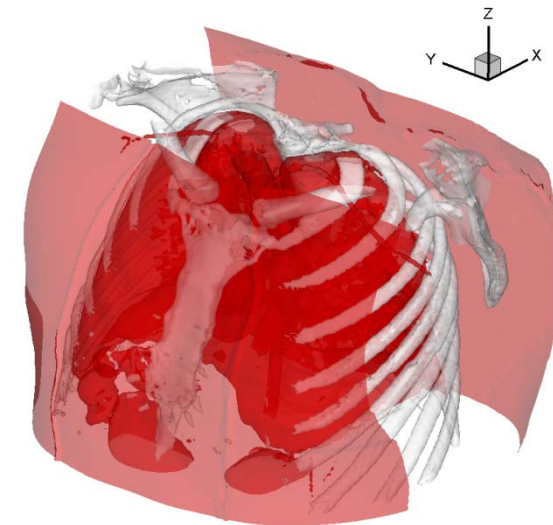
CT scan data
(Visible Human)



Material property
(density and speed of sound)
mapping



3D model of the thorax
(density iso-surfaces)



Cited Paper - Hemoacoustics

- Jung Hee Seo, Vijay Vedula, Theodore Abraham, and Rajat Mittal, “Multiphysics computational models for cardiac flow and virtual cardiography”, *Int. J. Num. Meth. Biomed. Eng.*, doi: 10.1002/cnm.2556, 2013.680, DOI: 10.1007/s10439-014-1018-4.
- Jung Hee Seo and Rajat Mittal, “A Coupled Flow-Acoustic Computational Study of Bruits from a Modeled Stenosed Artery”, *Medical & Biological Engineering & Computing*, Vol 50(10) pp 1025-35, 2012.
- Andreou, A.G.; Abraham, T.; Thompson, W.R.; Jung Hee Seo; Mittal, R., “Mapping the cardiac acoustome: An overview of technologies, tools and methods,” *Information Sciences and Systems (CISS)*, 2015 49th Annual Conference on , vol., no., pp.1,6, 18-20 March 2015, doi: 10.1109/CISS.2015.7086899
- Bakhshae, H.; Garreau, G.; Tognetti, G.; Shoele, K.; Carrero, R.; Kilmar, T.; Chi Zhu; Thompson, W.R.; Jung Hee Seo; Mittal, R.; Andreou, A.G., “Mechanical design, instrumentation and measurements from a hemoacoustic cardiac phantom,” *Information Sciences and Systems (CISS)*, 2015 49th Annual Conference on , vol., no., pp.1,5, 18-20 March 2015, doi: 10.1109/CISS.2015.7086901.
- Jung Hee Seo and Rajat Mittal, “A Coupled Flow-Acoustic Computational Study of Bruits from a Modeled Stenosed Artery”, *Medical & Biological Engineering & Computing*, Vol 50(10) pp 1025-35, 2012.
- J. H. Seo and R. Mittal, “A Higher-Order Immersed Boundary Method for acoustic wave scattering and low-Mach number flow-induced sound in complex geometries”, *Journal of Computational Physics*, 2011, Vol. 230, Issue 4, pp. 1000-1019 .
- Jung Hee Seo, Vijay Vedula, Theodore Abraham, and Rajat Mittal, “Multiphysics computational models for cardiac flow and virtual cardiography”, *Int. J. Num. Meth. Biomed. Eng.*, doi: 10.1002/cnm.2556, 2013.680,